Materials Chemistry and Physics 143 (2013) 271–274

Contents lists available at ScienceDirect

Materials Chemistry and Physics

journal homepage: www.elsevier.com/locate/matchemphys

Structure and properties of gas-nitrided nanostructured FeAlMnC alloy

Po-Chih Chen [a], Chuen-Guang Chao [a], Jenh-Yih Juang [b], Tzeng-Feng Liu [a,*]

[a] Department of Materials Science and Engineering, National Chiao Tung University, Hsinchu, Taiwan
[b] Department of Electrophysics, National Chiao Tung University, Hsinchu, Taiwan

HIGHLIGHTS

- AlN layer and aging effect are obtained in FeAlMnC alloy by one-step gas nitriding.
- Surface hardness reaching 1700 Hv and pitting potential above +1.7 V are attained.
- Nitrided layer is coherent and adhesive to the ductile matrix after tensile test.
- Gas nitriding is less sensitive to corner effect than the plasma nitriding process.

ARTICLE INFO

Article history:
Received 16 August 2013
Received in revised form
29 August 2013
Accepted 31 August 2013

Keywords:
Alloys
Nanostructures
Nitrides
Interfaces

ABSTRACT

The as-quenched Fe–9Al–28Mn–1.8C (in wt.%) alloy was directly gas-nitrided at 500 °C for 8 h, resulting in a ~30 μm-thick nitrided layer. The nitrided layer consists predominantly of nano-crystalline AlN with a small amount of Fe_4N. The nitrogen concentration at surface was extremely high up to ~17 wt.% (~41 at.%). Consequently, the surface microhardness (1700 Hv), substrate hardness (550 Hv), ductility (33.2%) and corrosion resistance in 3.5% NaCl solution of the present gas-nitrided alloy are far superior to those obtained previously for the optimally gas-nitrided or plasma-nitrided high-strength alloy steels, as well as martensitic and precipitation-hardening stainless steels. Moreover, it is very novel that the nitrided layer almost remained coherent and adhered well with the matrix after tensile test. Additionally, the present gas nitriding appeared to overcome the edge effects commonly encountered in plasma nitriding treatments for metals.

1. Introduction

The austenitic Fe–Al–Mn–C quaternary alloys having an excellent combination of strength and ductility, are promising materials for a wide variety of lightweight structural applications. Previously, we reported that the as-quenched microstructure of the Fe–9Al–28Mn–1.8C alloy was single-phase austenite (γ) containing an extremely high density of nano-sized κ′-carbides formed within γ-matrix by spinodal decomposition during quenching [1]. Due to the pre-existing nano-sized κ′-carbides, the aging time required for attaining the optimal combination of strength and ductility was much less than that of the previous Fe–Al–Mn–C with C ≦1.3 alloys [1–3]. Additionally, with almost equivalent elongation, the alloy aged at 450 °C for 12 h can possess yield strength about 28% higher than that of the optimally aged Fe–Al–Mn–C with C ≦1.3 alloys. Recently, in order to simultaneously harvest the excellent combination of strength and ductility as well as good corrosion resistance for applications in aggressive environments, plasma nitriding was carried out on a Fe–8.68Al–30.5Mn–1.85C alloy at 500 °C for 8 h [4]. Consequently, unprecedented results of the surface microhardness (1860 Hv), substrate hardness (550 Hv), ductility (33.6%) and pitting potential in 3.5% NaCl solution (+2030 mV) were obtained [4]. However, since plasma nitriding is susceptible to generate a negative glow zone of plasma discharge induced by the edge effect, it is generally unfavorable for components with sharp edges or complicated shapes [5,6]. In this respect, gas nitriding processes not only are characterized by relatively low cost and comparatively higher ecological safety, but also are more thermodynamically stable with more predictable conditions [7,8], thus are suitable for treating components of virtually any size and shape. To the best of our knowledge, little information is available concerning gas nitriding of Fe–Al–Mn–C alloys. Therefore, the aim of this work is to investigate the characteristics of gas-nitrided Fe–9Al–28Mn–1.8C alloy.

* Corresponding author. Tel.: +886 3 5131288; fax: +886 3 5713987.
E-mail address: tfliu@cc.nctu.edu.tw (T.-F. Liu).

0254-0584/$ – see front matter
http://dx.doi.org/10.1016/j.matchemphys.2013.08.063

2. Experimental

The details of preparation and pre-treatment conditions of the present Fe–9Al–28Mn–1.8C alloy prior to the gas nitriding were the same as those practiced in our previous work [4]. The gas nitriding process was performed at 500 °C for 8 h using an atmosphere of 50% N_2 and 50% H_2. Scanning electron microscopy (SEM) was used to investigate the surface and cross-sectional morphologies of the nitrided alloy before and after tensile test. X-ray diffraction (XRD) was carried out using a Bruker D8 with Cu-K_α radiation ($\lambda = 0.154$ nm). The nitrogen concentration and microhardness of the nitrided alloy were determined by using glow discharge spectrometer (GDS) and Vicker's indenter at 100 gf, respectively. The corrosion resistance measurement and tensile test were performed using the same setups and conditions as those used in Ref. [4].

3. Results and discussion

Fig. 1(a) is the cross-sectional SEM image of the present gas-nitrided alloy, revealing that the nitrided layer is ~30 μm-thick with the top-most 2 μm exhibiting very white appearance. It is noteworthy that the thickness of the present gas-nitrided layer is thinner than that obtained in previous plasma-nitrided alloy (~40 μm) [4]. It has been well-established that when performing gas and plasma nitriding, respectively, on alloys containing nitride-forming elements (e.g. Al, Cr) under the same treatment conditions (i.e. same time and temperature), the nitrided layer obtained in plasma nitriding was always thicker than in gas nitriding; whereas the reverse result was obtained for alloys without nitride-forming elements [9]. The inset image in Fig. 1(a) is an enlarged microstructure contiguous to interface between the nitrided layer and γ matrix. The average size of κ′-carbides has increased to ~25 nm, which is similar to what is expected for attaining optimal combination of mechanical properties for the Fe–9Al–28Mn–1.8C alloy [4]. Indeed, the ultimate tensile stress (UTS), yield strength (YS), and elongation (El) of the present gas-nitrided alloy are 1390 MPa, 1292 MPa, and 33.2%, respectively, The results are comparable to those obtained for the same alloy after being plasma nitrided at 500 °C for 8 h (1402 MPa, 1298 MPa, and 34.5%) [4]. Fig. 1(b) shows the elemental mapping in the rectangular region marked in Fig. 1(a). The results clearly delineate that Al has diffused outward and accumulated in the vicinity of surface to interact with inward-diffusing N. On the contrary, the concentrations of Fe and Mn in the nitrided layer appear to be less than those in the γ-matrix. The XRD results shown in Fig. 1(c) reveal that the nitrided layer is composed predominantly of nano-crystalline AlN (5–10 nm) with a small amount of Fe_4N. Moreover, the diffraction peaks of the γ-phase appear to be significantly broadened and shift to the lower diffraction angles, indicative of strained and expanded lattice arising from nitrogen incorporation [10]. This is similar to that observed previously in plasma nitriding of the same alloy [4].

Fig. 2(a) shows the depth-dependence of nitrogen concentration and microhardness of the gas-nitrided alloy. The nitrogen concentration at the surface is about 17 wt.% (~41 at.%) with microhardness 1700 Hv, and both exhibit an apparent plateau within the first several μm. The potentiodynamic polarization curve for the gas-nitrided alloy in 3.5% NaCl solution is shown in Fig. 2(b). Evidently, for the untreated alloy, there is no apparent passivation region. The corrosion current density (i_{corr}) and corrosion potential (E_{corr}) are 2×10^{-6} A cm^{-2} and −790 mV, respectively The corrosion current density (I_{corr}), corrosion potential (E_{corr}), pitting corrosion current density (I_p), pitting potential (E_{pit}) and $\Delta E(E_{pit} - E_{corr})$ were measured to be 5×10^{-6} A cm^{-2}, +25 mV, 9×10^{-9} A cm^{-2}, +25 mV and +1710 mV, respectively. Evidently, the surface microhardness and corrosion resistance behavior of the gas-nitrided alloy are slightly lower than those obtained by plasma nitriding [4]. The slight differences in surface hardness and corrosion resistance are due to the differences in thickness and compositions of the nitrided layer. Nevertheless, we emphasize here that such values of microhardness and corrosion resistance are still far superior to those obtained in optimally nitrided high-strength alloy steels, martensitic and precipitation-hardening stainless steels [4,10–12]; In these high-strength body-centered cubic (bcc)

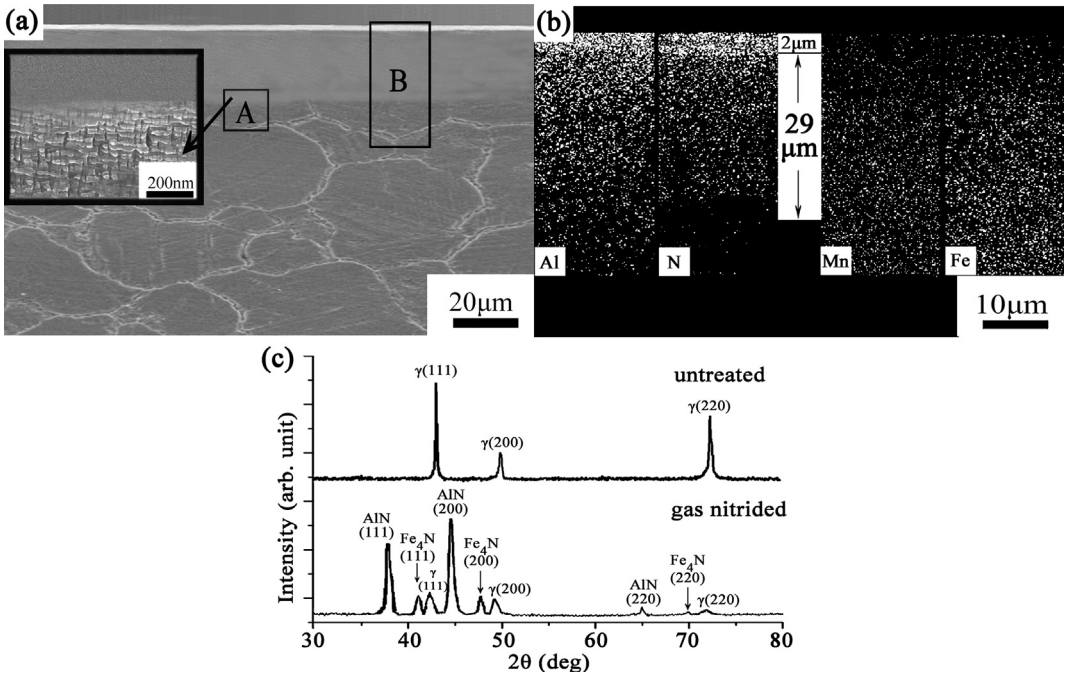

Fig. 1. (a) SEM cross-sectional image of the gas-nitrided alloy. Inset image shows the enlarged microstructure near the interface. (b) The images of elemental mapping in the rectangular region marked in (a). (c) XRD results for as-quenched and nitrided alloys.

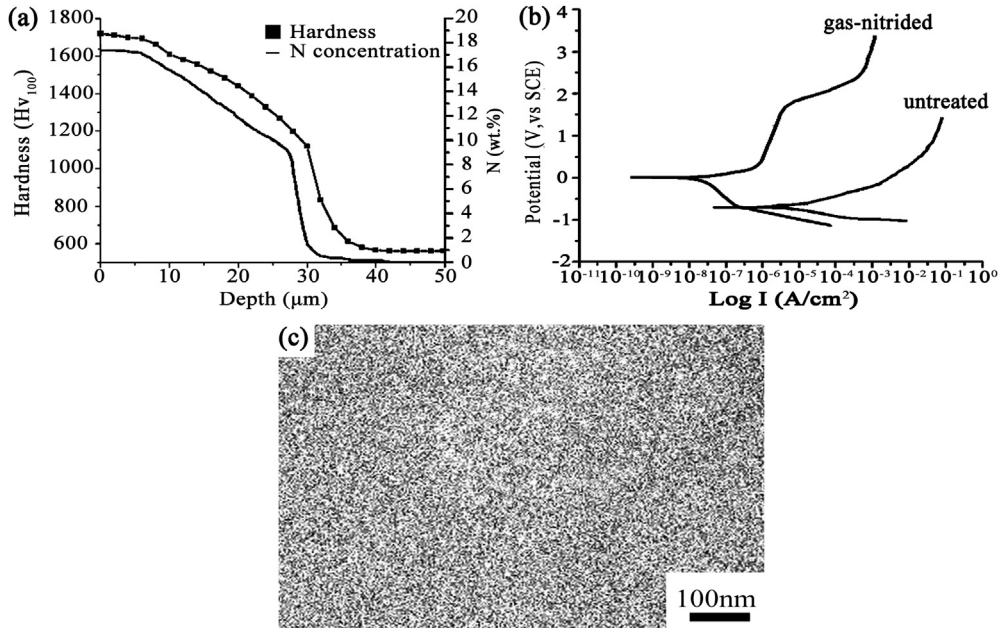

Fig. 2. (a) Nitrogen concentration and hardness profiles of the present gas-nitrided alloy. (b) Polarization curves for the untreated and present gas-nitrided alloys in 3.5% NaCl solution. (c) SEM surface image of the gas-nitrided alloy.

steels, the nitrided layer is mainly composed of Fe_3N (hexagonal close packed, hcp) and Fe_4N (fcc), without or with a trace of CrN (fcc), and the surface nitrogen concentration is in the range of 10–15 wt.% [13–15]. It is known that higher nitrogen concentration and dense packing of finer nitride particles can considerably improve the surface hardness and corrosion resistance of the nitrided alloys [13–15]. Fig. 2(c) clearly indicates that the surface of the nitrided layer consists of very dense and extremely fine AlN nitride particles, which on combining with the high nitrogen concentration near the surface thus explained the excellent properties of the present gas-nitrided alloy.

Next we will discuss the fracture behaviors of the nitrided layer, which have been largely ignored, despite that both gas and plasma nitriding have been ubiquitously applied to metal alloys, for improving surface microhardness and corrosion resistance. Fig. 3(a) is a SEM image taken from the free surface of the nitrided-alloy after tensile test. There are several salient features to be noted: (1) the nitrided layer deforms commensurately with the underneath γ-matrix along the direction of applied stress; (2) the top-most nitrided layer fractures evenly with cracks running perpendicular to the stress direction; (3) the fractured fragments do not spall and detach from the substrate; (4) the fractured layer is ~1.7 μm-deep (inset AFM image in Fig. 3(a)), which is consistent with the thickness of the white thin layer seen in Fig. 1(a); (5) the wavy morphology of the fractured layer also suggests that even AlN layer is not completely brittle, presumably due to the uniform nano-sized microstructure and/or substantial nitrogen concentration existing in this layer is less than that of the stoichiometric AlN (N ~ 50 at.%). Moreover, the tilted SEM image shown in Fig. 3(b) revealing simultaneously the free and fracture surfaces indicates that there are high density of dimples existing within the γ + κ′-carbides matrix, while no microvoids or microcracks can be observed in the vicinity of the interface, albeit the fracture surface of the nitrided layer does not contain as many dimples typical for ductile deformation. The coherent deformation and excellent adhesion between the nitrided layer and substrate may be attributed to the fact that AlN, Fe_4N, γ-matrix and κ′-carbides all are having the same fcc crystal structure with very similar lattice parameters [4]. Finally, we turn to the edge effect on gas nitriding process. Fig. 4 shows a typical gas-nitrided layer around a sharp sample corner. Clearly, the thickness of the nitrided layer around the corner is thicker than that of the nearby straight regions, which is in contrast to what is usually seen in plasma nitriding [6], suggesting that gas nitriding maybe more favorable for processing components with sharp edges and complicated shapes.

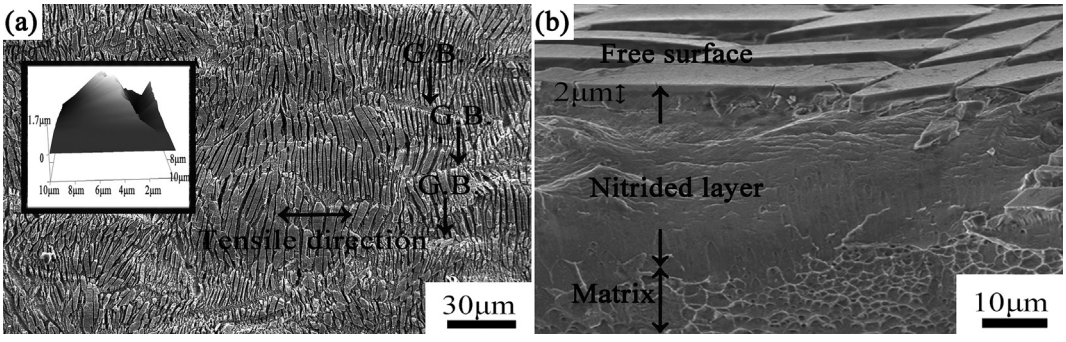

Fig. 3. (a) SEM image of the free surface of gas-nitrided alloy after tensile test. Inset image shows the AFM image of one of the fractured fragment. (b) SEM image of the fractured surface taken by slightly tilting the sample.

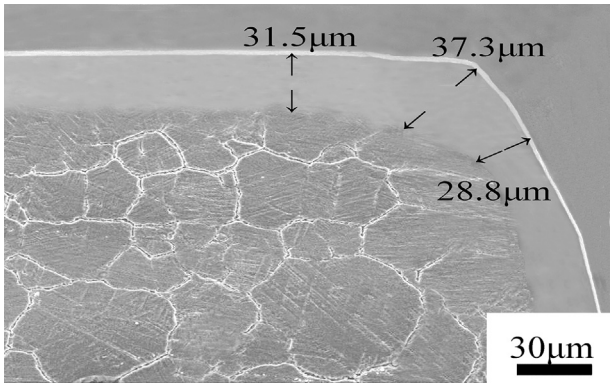

Fig. 4. SEM image of the nitrided layer near the corner.

4. Conclusions

Due to containing high content of strong nitride-forming element Al, the nitrided layer consists predominantly of nano-crystalline AlN with a small amount of Fe_4N in the present Fe–9Al–28Mn–1.8C alloy after being gas-nitrided at 500 °C for 8 h, the resultant nitrided layer accounts for the large surface microhardness (~ 1700 Hv), and the superior corrosion resistance in 3.5% NaCl solution, as well as the coherent and adhesive fracture behavior obtained. Moreover, gas nitriding appears to yield more uniform nitrided layer without suffering the edge effects.

Acknowledgments

This work was supported by the National Science Council, Taiwan (NSC-100-2221-E-009-053-MY3).

References

[1] K.M. Chang, C.G. Chao, T.F. Liu, Script. Mater. 63 (2010) 162.
[2] W.K. Choo, J.H. Kim, J.C. Yoon, Acta Mater. 45 (1997) 4877.
[3] I. Kalashnikov, O. Acselrad, A. Shalkevich, L.C. Pereira, J. Mater. Eng. Perform. 9 (2000) 597.
[4] P.C. Chen, C.G. Chao, T.F. Liu, Script. Mater. 68 (2013) 380.
[5] P. Kochmanski, J. Nowacki, Surf. Coat. Technol. 202 (2008) 4834.
[6] S.D. de Souza, M. Kapp, M. Olzon-Dionysio, M. Campos, Surf. Coat. Technol. 204 (2010) 2976.
[7] J. Bielawski, J. Baranowska, K. Szczecinski, Surf. Coat. Technol. 200 (2006) 6572.
[8] Yucel Birol, Eng. Fail. Anal. 26 (2012) 203.
[9] F. Ashrafizadeh, Surf. Coat. Technol. 173–174 (2003) 1196.
[10] C.X. Li, T. Bell, Corros. Sci. 48 (2006) 2036.
[11] Y. Li, L. Wang, D. Zhang, L. Shen, Appl. Surf. Sci. 256 (2010) 4149.
[12] R.F. Liu, M.F. Yan, Mater. Des. 31 (2010) 2355.
[13] W.P. Tong, N.R. Tao, Z.B. Wang, J. Lu, K. Lu, Science 299 (2003) 686.
[14] G.J. Li, J. Wang, Q. Peng, C. Li, Y. Wang, B.L. Shen, J. Mater. Process. Technol. 207 (2008) 187.
[15] C.X. Li, T. Bell, Corros. Sci. 46 (2004) 1527.